



Increased carbon capture by a silicate-treated forested watershed affected by acid deposition

Lyla L. Taylor^{1*}, Charles T. Driscoll², Peter M. Groffman³, Greg H. Rau⁴, Joel D. Blum⁵ and David J. Beerling¹

5 ¹Leverhulme Centre for Climate Change Mitigation, Department of Animal and Plant Sciences, University of Sheffield, Sheffield S10 2TN, UK

²Department of Civil and Environmental Engineering, 151 Link Hall, Syracuse University, Syracuse, NY 13244, USA

³City University of New York, Advanced Science Research Center at the Graduate Center, New York, NY 10031 and Cary Institute of Ecosystem Studies, Millbrook, NY 12545 USA

10 ⁴Institute of Marine Sciences, University of California, Santa Cruz, CA 95064 USA

⁵Department of Earth and Environmental Sciences, University of Michigan, Ann Arbor, MI 48109, USA

Correspondence to: Lyla L. Taylor (L.L.Taylor@sheffield.ac.uk)

Abstract. Meeting internationally agreed-upon climate targets requires Carbon Dioxide Removal (CDR) strategies coupled with an urgent phase-down of fossil fuel emissions. However, the efficacy and wider impacts of CDR are poorly understood.

15 Enhanced rock weathering (ERW) is a land-based CDR strategy requiring large-scale field trials. Here we show that a low 3.44 t ha⁻¹ wollastonite treatment in an 11.8-ha acid-rain-impacted forested watershed in New Hampshire, USA led to cumulative carbon capture by carbonic acid weathering of 0.025–0.13 t CO₂ ha⁻¹ over 15 years. Despite a 0.8–2.4 t CO₂ ha⁻¹ logistical carbon penalty from mining, grinding, transportation and spreading, by 2015 weathering together with increased forest productivity led to net CDR of 8.5–11.5 t CO₂ ha⁻¹. Our results demonstrate that ERW may be an effective, scalable

20 CDR strategy for acid-impacted forests but at large-scale requires sustainable sources of silicate rock dust.

1 Introduction

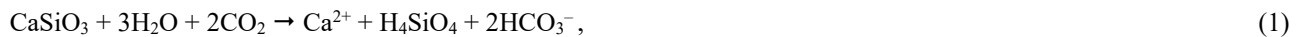
The Intergovernmental Panel on Climate Change (IPCC)(Rogelj et al., 2018) Special Report on global warming indicates large-scale deployment of Carbon Dioxide Removal (CDR) technologies will be required to avoid warming in excess of 1.5 °C by the end of this century. Land-based CDR strategies include enhanced rock weathering (ERW), which aims to accelerate 25 the natural geological process of carbon sequestration by amending soils with crushed reactive calcium (Ca) and magnesium (Mg)-bearing rocks such as basalt (The Royal Society and The Royal Academy of Engineering, 2018;Hartmann et al., 2013). Forests represent potential large-scale deployment opportunities where rock amendments may provide a range of benefits, including amelioration of soil acidification and provisioning of inorganic plant-nutrients to cation-depleted soils (Hartmann et al., 2013;Beerling et al., 2018). Although ERW has not yet been demonstrated as a CDR technique at the catchment scale, a 30 forested watershed experiment at the Hubbard Brook Experimental Forest (HBEF, 43° 56'N, -71° 45'E) in the White



Mountains of New Hampshire, USA provides an unusual opportunity for assessing proof-of-concept in this priority research area.

The HBEF watershed experiment, designed to restore soil calcium following decades of leaching by acid rain, involved application of a finely ground rapidly-weathered calcium silicate mineral wollastonite (CaSiO_3 ; 3.44 t ha^{-1}) on 19 October 35 1999 to an 11.8-ha forested watershed (SI Appendix) (Likens et al., 2004; Peters et al., 2004; Shao et al., 2016). Unlike the carbonate minerals (e.g., CaCO_3) commonly applied to acidified soils (Lundström et al., 2003), wollastonite does not release CO_2 when weathered (Supplementary Information) so is much better suited for CDR (Hartmann et al., 2013). It also has dissolution kinetics comparable to or faster than other calcium-rich silicate minerals such as labradorite found in basalt (Brantley et al., 2008). Thus, the HBEF experiment provides a timely and unparalleled opportunity for investigating the long-term (15 years) effects of ERW on CDR potential via forest and stream water chemistry responses. 40

In the case of ERW with wollastonite, CDR follows as Ca cations (Ca^{2+}) liberated by weathering consume atmospheric CO_2 through the formation of bicarbonate (HCO_3^-) by charge balance, as described by the following reaction:



However, forests in the northeastern USA have experienced acid deposition (Likens and Bailey, 2014), changes in 45 nitrogen cycling (Goodale and Aber, 2001; McLauchlan et al., 2007) and increases in dissolved organic carbon (DOC) fluxes (Cawley et al., 2014) that may affect CO_2 removal efficiency by ERW processes. In particular, CO_2 consumption as measured by bicarbonate production may be diminished if sulphate (SO_4^{2-}), nitrate (NO_3^-), or naturally-occurring organic acid anions (Fakhraei and Driscoll, 2015) (H_2A^-) in DOC intervene to inhibit the following mineral weathering reactions. For example:



These environmental effects on stream-water chemistry are well documented at the HBEF (Cawley et al., 2014; Likens and Bailey, 2014; Rosi-Marshall et al., 2016; McLauchlan et al., 2007), and may be exacerbated under future climate change (Sebestyen et al., 2009; Campbell et al., 2009).

55 Here we exploit the experimental design and long-term monitoring of streamwater chemistry, trees, and soils, for two small forested HBEF watersheds to evaluate the effects of the wollastonite treatment in 1999 on catchment CO_2 consumption via inorganic and organic pathways. Further, we examine how biogeochemical perturbations in S, N, and organic carbon cycling affect catchment inorganic CO_2 consumption. We consider the forest response, the carbon cost for ERW deployment (mining, grinding, transportation and application), and the net greenhouse gas balance for the treatment. Finally, we provide 60 an initial assessment of the net CDR potential of silicate treatments deployed over larger areas of acidified forest in the northeastern United States.



2 Methods

2.1 Site and treatment

2.1.1 Site description

65 The HBEF has a temperate climate with ~1400 mm mean annual precipitation of which up to one third falls as snow (Campbell et al., 2007). The mean temperatures in January and July are -9°C and 18°C respectively, and the period from mid-May to mid-September comprises the growing season (Campbell et al., 2007). There are six small southeast-facing watersheds in the HBEF with 20%–30% slopes (Groffman et al., 2006), including a biogeochemical reference (watershed W6, 13.2 ha, 545–791m asl) and one which received the silicate treatment (watershed W1, 11.8 ha, 488–747m asl). Carbonate and evaporite minerals are in very low abundance (<1% calcite in the crystalline rocks and glacial deposits) in these silicate-mineral dominated watersheds (Johnson et al., 1981). Well-drained Typic Haplorthod soils with $\text{pH} < 4.5$ and mean depth 0.6m formed from relatively impermeable glacial till, which restricts water flow and protects the underlying schist bedrock from weathering. Overland runoff and flow through bedrock are both thought to be negligible (Likens, 2013). Hydrologically, the HBEF watersheds are typical of small catchments in northern New England (Sopper and Lull, 1965). Flow rates for W1 and W6 75 along with streamwater pH are shown in Fig. S1. Prior to treatment, streamwater calcium concentrations were under $30 \mu\text{mol L}^{-1}$ while bicarbonate concentrations were under $5 \mu\text{mol L}^{-1}$, below the ranges for typical world rivers (Moon et al., 2014) (60 – $2293 \mu\text{mol Ca}^{2+} \text{ L}^{-1}$, 179 – $4926 \mu\text{mol HCO}_3^- \text{ L}^{-1}$).

76 *Fagus grandifolia*, *Betula allegheniensis* and *Acer saccharum* are the dominant trees in this Northern Hardwood forest, while *Betula papyrifera*, *Abies balsamea* and *Picea rubens* are common at the highest elevations where soils tend to be shallow 80 and wetter (Cho et al., 2012). *A. saccharum* and *P. rubens* are both calcium-sensitive, but soil calcium-bearing minerals are less available to *A. saccharum* (Blum et al., 2002) and total bioavailable calcium content decreases with elevation (Cho et al., 2012). This silicate-addition experiment was designed to replace bioavailable calcium which had been stripped from the soils by decades of acid deposition.

2.1.1 Treatment description

85 On 19 and 21 October 1999, W1 was treated with 344 g/m^2 of pelletized wollastonite (CaSiO_3) by a GPS-equipped helicopter with a motorized spreader to ensure even deployment across the catchment, including the 1804 m^2 streambed (Peters et al., 2004). Following treatment, the lignin-sulfonate binder forming the pellets dissolved within several days (Peters et al., 2004), and the ground wollastonite itself dissolved rapidly in the upper Oie soil horizon, increasing Oie base saturation from 40% to 78% and raising soil pH from 3.88 to 4.39 within one year (Johnson et al., 2014). Although the budget of wollastonite-derived 90 calcium (Wo-Ca) has never been closed due to lack of data from vegetation and from deeper soil layers (Shao et al., 2016), it



is thought that uptake by vegetation and retention by soil exchange sites delayed transport of Wo-Ca to lower soil horizons and streamwater for three years (Johnson et al., 2014).

2.2 Modelling approach

2.2.1 Forward modelling of streamwater chemistry including dissolved inorganic carbon

95 We used a forward modelling approach to calculate dissolved streamwater bicarbonate concentrations ($[\text{HCO}_3^-]_{\text{stream}}$) in the treated and reference watersheds over ~25 years, including 15 years post-treatment, with the United States Geological Survey (USGS) aqueous geochemistry software PHREEQC version 3.3.12-12704 (Parkhurst and Appelo, 1999) and monthly long-term (1992–2014) streamwater (Driscoll, 2016a, b) and rain/snow precipitation (Likens, 2016b, a) chemistry measurements.

100 Using MATLAB (version R2016a) scripts, we wrote PHREEQC input files and determined the inorganic carbon species for each streamwater sample with PHREEQC. Along with a standard database which decouples ammonium and nitrate (Amm.dat, provided with the PHREEQC software), we included the ionization constants for the organic acid triprotic analogue and the constants for Al complexation described for Hubbard Brook streams (Fakhraei and Driscoll, 2015) in our PHREEQC simulations. These are: $\text{pK}_{\text{a1}}=2.02$, $\text{pK}_{\text{a2}}=6.63$, $\text{pK}_{\text{a3}}=7.30$, $\text{pK}_{\text{Al1}}=4.07$, $\text{pK}_{\text{Al2}}=7.37$, $\text{pK}_{\text{Al3}}=6.65$, and site density $m=0.064 \text{ mol sites mol C}^{-1}$. Our organic acid concentrations are the product of the corresponding site density of reactions and the measured 105 dissolved organic carbon concentration (Fakhraei and Driscoll, 2015); these were PHREEQC inputs along with total monomeric Al and major ion concentrations from the longitudinal datasets.

110 Spectator ions (Cl^- and NH_4^+) were adjusted to achieve charge balance given the measured pH for the treated and reference watersheds. Cl^- was only adjusted when charge balance was not achieved using NH_4^+ alone. This was deemed to be the case when PHREEQC failed to converge or when the percent error exceeded 5%. We used original rather than adjusted rainwater Cl to calculate the contribution of rainwater to streamwater chemistry (described below). These adjusted ions were then held constant for our modelled scenarios, while pH was allowed to vary.

115 Exploratory PHREEQC tests (charge-balancing on DIC) either with or without organic acids suggest that the acids depress total DIC, HCO_3^- and also the saturation state of gaseous CO_2 . Similar variability in the saturation is also observed when DIC values from partially degassed samples from the streams are used as input. We chose minimum and maximum values of 1100 and 1700 ppm, or ~3 and 4.6×368 , the mean value of Mauna Loa pCO_2 for 1985–2012. These values correspond to $\log_{10}(\text{pCO}_2(\text{g})) = -2.87 \pm 0.09 \text{ SD}$ derived from a prior analysis of this variability for the same time range (Fakhraei and Driscoll, 2015).

2.2.2 Streamwater temperature

120 Air temperatures for the Hubbard Brook watersheds (Campbell, 2016) were converted to streamwater temperatures following Mohseni and Stefan (Mohseni and Stefan, 1999). Rainwater temperatures were set equal to streamwater



temperatures. These temperatures were used in our PHREEQC modelling, with equilibrium constants for the DIC species as functions of temperature. Only samples measured closest to the weirs and with a valid pH were processed with PHREEQC.

2.2.3 Catchment CO₂ consumption

Annual total watershed CO₂ consumption (Eq. 1) was calculated as the product of streamwater flow and [HCO₃⁻]_{stream}, 125 corrected for the HCO₃⁻ contribution of rainwater ($\alpha_{\text{rain},\text{HCO}_3}$, see below), as given by:

$$\text{CO}_{2,\text{HCO}_3}(t) = [\text{HCO}_3^-]_{\text{weath}}(t) \times \text{flow} = (1 - \alpha_{\text{rain},\text{HCO}_3,t}) [\text{HCO}_3^-]_{\text{stream}}(t) \times \text{flow}, \quad (5)$$

where [HCO₃⁻]_{stream} is given in mol kgw⁻¹ and flow is the “runoff” in mm time⁻¹. Calculated [HCO₃⁻]_{stream} and annual CO₂ consumption for the treated and reference watersheds (Eqs. 5 and 13) comprise our baseline simulations and represent a primary test of hypothesized increased carbon capture resulting from weathering of the applied silicate.

130 To isolate a treatment effect for bicarbonate, we used strontium isotopes as a tracer of wollastonite (Wo) weathering within a previously-published mixing function (Nezat et al., 2010; Peters et al., 2004) (Methods, **Fig. S3**). This mixing function provides the fraction X of calcium originating from wollastonite. The contribution of all mineral sources other than wollastonite to CO₂ consumption (Eq. 5) is simulated by running simulations with Ca²⁺ concentrations reduced by (1- X):

$$\text{Non-Wo-CO}_{2,\text{HCO}_3}(t) = [\text{HCO}_3^-]_{\text{stream}}(t, (1-X)\text{Ca}) \times (1 - \alpha_{\text{rain},\text{HCO}_3,t}) \times \text{flow}(t), \quad (6)$$

135 where α_{rain} is the fractional contribution from rain/snow precipitation (Methods). The treatment effect is then the difference between Eq. (5) and Eq. (6):

$$\begin{aligned} \text{Wo-CO}_{2,\text{HCO}_3}(t) &= ([\text{HCO}_3^-]_{\text{stream}}(t, \text{Ca}) - [\text{HCO}_3^-]_{\text{stream}}(t, (1-X)\text{Ca})) \times (1 - \alpha_{\text{rain},\text{HCO}_3,t}) \times \text{flow}(t) \\ &= \text{CO}_{2,\text{HCO}_3}(t) - \text{Non-Wo-CO}_{2,\text{HCO}_3}(t), \end{aligned} \quad (7)$$

140 Bicarbonate-derived CO₂ consumption (Eq. 5) is the most conservative approach to estimating net carbon fluxes related to ERW. For natural freshwaters in equilibrium with the atmosphere, this entails a titration for total alkalinity with a possible correction for the concentration of organic acid anions (Köhler et al., 2000). However, another widely used (Jacobson and Blum, 2003) measure of CO₂ consumption is derived assuming charge-balance of base cations (Ca²⁺, Mg²⁺, K⁺ and Na⁺) by bicarbonate formation (Eq. 1)

$$\begin{aligned} 145 \text{CO}_{2,\text{ions}}(t) &= (2[\text{Ca}^{2+}](1 - \alpha_{\text{rain},\text{Ca},t}) + 2[\text{Mg}^{2+}](1 - \alpha_{\text{rain},\text{Mg},t}) + [\text{K}^+](1 - \alpha_{\text{rain},\text{K},t}) + \\ &\quad [\text{Na}^+](1 - \alpha_{\text{rain},\text{Na},t}) - 2[\text{SO}_4^{2-}](t)) \times \text{flow}, \end{aligned} \quad (8)$$

where streamwater cation equivalents are corrected for contributions from rain/snow precipitation (Methods) and sulphuric acid weathering (Chetelat et al., 2008) (Eq. 2). For an ERW treatment, transient changes in the export of ions not derived from



the applied minerals may occur, but we consider that the cations released from the applied minerals comprise the most
 150 unambiguous treatment effect. The charge associated with wollastonite-derived Ca^{2+} (Wo-Ca) determines the CO_2 consumption associated with the HBEF wollastonite treatment:

$$\text{Wo-CO}_{2,\text{Ca}}(t) = 2 \times X \times [\text{Ca}^{2+}](t) \times \text{flow}(t), \quad (9)$$

where X is the fraction of Ca^{2+} from weathered wollastonite. Equations 8 and 9 are optimistic measures of CO_2 consumption because they ignore both the weathering agent and streamwater inorganic carbon, assuming charge-balance of cations by carbonate and bicarbonate ions in the oceans. Eqs. 7 and 9, together with our flux calculations accounting for sparsity of concentration data compared to daily flow data (Methods), should help avoid major uncertainties in catchment-scale CO_2 consumption calculations: the provenance of the cations and variations in concentration and discharge (Moon et al., 2014).

2.2.4 Fraction of calcium derived from wollastonite

We applied a two-component mixing model that had previously been developed by Peters et al (Peters et al., 2004):

$$160 \quad X_{\text{Ca}} = \left[\frac{\left(\frac{^{87}\text{Sr}}{^{86}\text{Sr}} \right)_{\text{post}} - \left(\frac{^{87}\text{Sr}}{^{86}\text{Sr}} \right)_{\text{pre}} \left(\frac{\text{Sr}}{\text{Ca}} \right)_{\text{pre}}}{\left(\left(\frac{^{87}\text{Sr}}{^{86}\text{Sr}} \right)_{\text{post}} - \left(\frac{^{87}\text{Sr}}{^{86}\text{Sr}} \right)_{\text{pre}} \right) \left(\frac{\text{Sr}}{\text{Ca}} \right)_{\text{pre}} + \left(\left(\frac{^{87}\text{Sr}}{^{86}\text{Sr}} \right)_{\text{Wo}} - \left(\frac{^{87}\text{Sr}}{^{86}\text{Sr}} \right)_{\text{pre}} \right) \left(\frac{\text{Sr}}{\text{Ca}} \right)_{\text{Wo}}} \right], \quad (10)$$

where pre-app and post-app refer to pre-application and post-application streamwater concentrations and Wo refers to wollastonite. The Sr data (Blum, 2019) have been extended through 2015. See SI Appendix for further discussion of the use of strontium and its isotopes as tracers of Ca^{2+} provenance.

2.2.5 Contributions of rain/snow precipitation to streamwater chemistry

165 We estimated the contribution of rain/snow (Likens, 2016b, a) relative to all other sources, using a previously published mixing model (Négrel et al., 1993). We assume all Cl^- in the water is from rain/snow, noting that this common treatment of Cl as an unreactive tracer is not always justified (Lovett et al., 2005). The contribution of precipitation to the streamwater (α_{rain}) is generally set using Na and Cl, which are less affected by nutrient cycling and adsorption than other major ions (Négrel et al., 1993):

$$170 \quad \alpha_{\text{rain,Na,t}} = \frac{[\text{Cl}]}{[\text{Na}]}(\text{stream,t}) / \frac{[\text{Cl}]}{[\text{Na}]}(\text{rain,t}), \quad (11)$$

To account for attenuation of the rain/snow precipitation leaching through the soil, Cl/Na and HCO_3/Na at any given time (t) are means from the previous three months. The contribution of rain/snow to other ions such as HCO_3^- in the streamwater can be estimated as follows:

$$175 \quad \alpha_{\text{rain,HCO}_3,t} = \alpha_{\text{rain,Na,t}} \times \frac{[\text{HCO}_3]}{[\text{Na}]}(\text{stream,t}) / \frac{[\text{HCO}_3]}{[\text{Na}]}(\text{rain,t}), \quad (12)$$



2.2.6 Flux calculations

To ensure that fluxes from our two watersheds were comparable and to correct for the sparsity of solute measurements compared to flow measurements, we created rolling annual flow-adjusted fluxes using Method 5 of Littlewood et al
180 (Littlewood et al., 1998) at five evenly-spaced points each year:

$$\text{Flux} = \text{scale} \times \left[\frac{\sum_{i=1}^M C_i Q_i}{\sum_{i=1}^M Q_i} \right] \times \left[\frac{\sum_{k=1}^N Q_k}{N} \right], \quad (13)$$

where Q_i is the measured instantaneous stream flow, C_i is the concentration for sample i , M is the number of streamwater chemistry samples in the year (usually 12), Q_k is the k^{th} flow measurement, and N is the number of flow measurements. In
185 our case, daily flow measurements (Campbell, 2015) and ~monthly streamwater samples (Driscoll, 2016a, b) were available. Therefore, the mean concentration for the preceding twelve months is multiplied by the mean flow for the same period, suitably scaled to get the total annual flux. Without sub-daily timestamps for the longitudinal streamwater chemistry data, we used daily total flows rather than instantaneous flows. Tests suggested that there was little difference between using mean daily instantaneous flows and the mean daily total flows.

190 2.3 Greenhouse gas balance

2.3.1 Carbon sequestration in wood

Battles et al (Battles et al., 2014) provided mean wood production over two five-year periods for the treated and reference watersheds. We considered the difference (treated-reference) to be an estimate of the treatment effect on potentially long-term biomass carbon sequestration. Assuming 46.5% of the woody biomass is carbon (Martin et al., 2018), our calculated
195 cumulative additional C sequestration in the treated watershed over ten years [given by $(5 \times 0.78 + 5 \times 0.29) \times 0.465 \times 100 / 12$] was $20.7 \text{ mol C m}^{-2}$ ($9.1 \text{ t CO}_2 \text{ ha}^{-1}$).

2.3.2 Greenhouse gas emissions from soils

Measurements (Groffman, 2016) were taken at four elevations in the treated watershed and at points just west of the reference watershed starting in 2002. Gas samples were collected from chambers placed on three permanent PVC rings at each of these
200 eight sites (Groffman, 2016). The data were not normally distributed so were analyzed with Kruskal-Wallis tests at the 0.05 significance level; however, tests with one-way ANOVA produced the same overall results. All analyses were done in Matlab R2016a.

Cumulative curves for each of the 24 chambers were generated by matching the dates of the measurements, excluding points which were missing data for any chamber and allowing up to a week's discrepancy between catchments. Nearly all
205 discrepancies were within one day. Assuming diurnal variation was minor compared to seasonal variation, each datum (g C



$\text{m}^{-2} \text{ hour}^{-1}$) was multiplied by 24 hours and by 30 days to get $\text{gC m}^{-2} \text{ month}^{-1}$. There was no extrapolation to fill gaps in the dataset; curves shown in Fig. 3 are internally consistent but not comparable to other datasets. We were particularly interested in the elevation-specific responses, as the different elevations have distinct tree species compositions and below-ground responses to the wollastonite treatment (Fahey et al., 2016).

210 The HBEF experimental watersheds are divided into $25 \times 25\text{m}$ plots on slope-corrected grids. Vegetation has been surveyed four times since the late 1990s and assigned a zone designation in each plot (Driscoll et al., 2015; Driscoll Jr et al., 2015; Battles et al., 2015b, a) (Supplementary Fig. S9). To estimate the respiration savings over the whole watershed, we added the areas of individual plots which were assigned to our four vegetation types (Low, Mid and High hardwoods, and Spruce-Fir). Because there were seven vegetation types in the datasets, we compared all types with pairwise Kruskal-Wallis 215 tests at the 0.05 significance level using the basal area data for the six dominant tree species. Kruskal-Wallis tests were appropriate because the data, and therefore the differences from the means (residuals), were not normally distributed. These tests suggested that the “extra” vegetation types (“Birch/Fern Glade”, and “Poor Hardwoods” at High and Mid elevations) could be combined with Spruce-Fir, High and Mid Hardwoods respectively. Watershed fractions for our combined forest types were 0.155 for SpruceFir, 0.16 for High Hardwoods, 0.415 for Mid Hardwoods, and 0.27 for Low Hardwoods. When creating 220 our composite treatment effects for the entire watershed, we considered a treatment effect to be present only where our statistical analyses suggested significantly different fluxes.

2.3.3 Logistical carbon emissions costs

We used the 1999 upstate New York CO_2 emission factor for electricity generation from oil (United States Environmental Protection Agency, 1999) ($0.9 \text{ Mg CO}_2 \text{ MWh}^{-1}$), and rearranged Equation 28 of Stamboliadis (Stamboliadis et al., 2009):

$$225 \quad e_p = \frac{\left[e^{\frac{(\ln s/\alpha)}{\mu}} \right]}{3600 \times 1000}, \quad (14)$$

230 where the specific surface area s ($1600 \text{ m}^2 \text{ kg}^{-1}$ for our treatment) is related to the specific potential energy e_p of the material (kJ kg^{-1}), with theoretical parameters (Stamboliadis et al., 2009) $\alpha=139 \text{ m}^2 \text{ kJ}^{-1}$ and $\mu=0.469$ (dimensionless). We convert this potential energy to $\text{MWh t}^{-1} \text{ Qz}$ (3600 seconds per hour and $1000 \text{ kWh MWh}^{-1}$). The equation was derived for quartz (Qz) which has hardness 7. Because wollastonite hardness is in the range 5–5.5, this equation may overestimate the energy needed to grind the wollastonite.

The main energy source in Allerton will have been coal, and the 1999 Illinois emissions factor (United States Environmental Protection Agency, 1999) is $1.1 \text{ Mg CO}_2 \text{ MWh}^{-1}$. The monetary cost is $\text{USD}0.041 \text{ kWh}^{-1}$ for pelletization of limestone fines and $\text{USD}0.85 \text{ t}^{-1}$ product, so we estimate 20.73 kWh t^{-1} product.

235 Road transport distances were estimated using Google Maps (1397 km Gouverneur to Allerton, 1757 km Allerton to Woodstock, 408 km Gouverneur to Woodstock). We used standard emissions ranges (Sims et al., 2014) for Heavy Duty Vehicles (HDVs) ($70\text{--}190 \text{ gCO}_2 \text{ km}^{-1} \text{ t rock}^{-1}$) and for short-haul cargo aircraft ($1200\text{--}2900 \text{ gCO}_2 \text{ km}^{-1} \text{ t}^{-1}$). Emissions for the



HBEF experiment are provided in Table 2 with calculation details given in Table 3. The Matlab script used for these calculations is available on request. Note: t refers to megagrams, not US short tons.

2.3.4 Greenhouse gas budget for a treatment

240 The success of any treatment for climate change mitigation is determined by the net greenhouse gas (CO₂ equivalent) fluxes prior to and following treatment, at the treatment site and downstream. The GHG balance associated with any treatment, including ERW, is given by

$$\Delta\text{GHG} = \Delta\text{NEP} + \Delta\text{CONS} + \Delta\text{CH4} - \Delta\text{N2O} - \Delta\text{NO3N2O} - \Delta\text{TOC} - \text{LOGOPEN}, \quad (15)$$

245 where the individual fluxes are described and values given in Table 2. Here, ΔTOC and ΔNO3N2O are penalties because these lead to CO₂ and N₂O emissions downstream.

Changes in net ecosystem productivity due to the treatment ΔNEP can be represented by

$$\Delta\text{NEP} = \Delta\text{biomass} + \Delta\text{SOC} - \Delta\text{SRESP} - \Delta\text{ARESP} \quad (16)$$

250 where SOC is soil organic carbon, SRESP is soil (root+heterotrophic) respiration and ARESP is aboveground (wood+canopy) respiration. For the HBEF wollastonite experiment, we lack belowground biomass and aboveground respiration. Wood is a longer-term carbon sink than leaves or twigs so we have chosen to let this represent our biomass increment. Eq. (15) neglects ecosystem disturbances including fire, and possible carbonate mineral precipitation in soils. There is no evidence for the latter at the HBEF.

With the exception of CO₂ consumption, treatment effects were calculated as the difference (treated-reference) between the two watersheds. We used a range of emissions factors for N₂O to estimate the penalty associated with nitrate export 255 (ΔNO3N2O); low: 0.0017 kgN₂O-N kg⁻¹ DIN (Hu et al., 2016) and high: 0.0075 kgN₂O-N kg⁻¹ DIN (De Klein et al., 2006), where DIN is dissolved inorganic nitrogen dominated by nitrate. This N₂O was then converted to CO_{2e} (CO₂ equivalents in terms of cumulative radiative forcing) given the 100-year time horizon global warming potential (Pachauri et al., 2014) (GWP₁₀₀) for N₂O: 265 gCO_{2e} g⁻¹ N₂O. Likewise, ΔCH4 was converted to CO_{2e} (CO₂ equivalents in terms of cumulative radiative forcing) given GWP₁₀₀ for CH₄: 28 gCO_{2e} g⁻¹ CH₄.

260 3 Results

3.1 Wollastonite treatment increased streamwater CO₂ export

We first consider the time-series of streamwater changes in Ca²⁺ concentrations in the treated ([Ca]_{T,stream}) and reference ([Ca]_{R,stream}) watersheds. Immediately after treatment, [Ca]_{T,stream} increased from <30 μmol L⁻¹ to ~60 μmol L⁻¹, and then slowly declined over the next decade, remaining persistently above [Ca]_{R,stream} for 15 years (Fig. 1a). The initial post-treatment peak 265 represents dissolution of wollastonite within the stream (Peters et al., 2004) and release of calcium from hyporheic exchange during the first few years (Shao et al., 2016; Nezat et al., 2010). Retention of Ca²⁺ ions liberated by wollastonite dissolution (Wo-Ca) in the watershed soils (Nezat et al., 2010) and sequestration into tree biomass (Balogh-Brunstad et al., 2008; Nezat et



al., 2010) delayed appearance in streamwater for three years (Shao et al., 2016; Nezat et al., 2010). Subsequently, $[\text{Ca}]_{\text{T,stream}}$ remained approximately double $[\text{Ca}]_{\text{R,stream}}$, with a ~30% contribution from non-wollastonite Ca^{2+} until 2012. Towards the 270 end of the time-series, increased seasonal NO_3^- export in the treated watershed between 2012 and 2014 (Rosi-Marshall et al., 2016) led to Wo-Ca displacing non-Wo-Ca from the soil exchanger.

We derived the annual export of Ca^{2+} from the treated and reference watersheds as the product of mean annual flow-adjusted Ca^{2+} streamwater concentrations and annual flow (**Fig. 1b**) (Methods). After accounting for variations in flow, increased streamwater Ca^{2+} concentrations in the treated watershed are translated into a 2-fold increase in total Ca^{2+} export 275 relative to the reference watershed that was maintained for 15 years until 2015 through this analysis period. Overall, the wollastonite treatment resulted in a sharp spike in calculated CO_2 consumption ($\text{Wo-CO}_{2,\text{Ca}}$) that decreased but remained elevated as a result of the treatment (**Fig. 1c**).

Temporal patterns in modelled streamwater bicarbonate concentration in both treated and reference watersheds (**Fig. 1d**), and the corresponding total annual CO_2 consumption ($\text{CO}_{2,\text{HCO}_3}$) (**Fig. 1e**) and CO_2 consumption resulting from treatment 280 ($\text{Wo-CO}_{2,\text{HCO}_3}$) (**Fig. 1f**), largely mirror changes in streamwater Ca^{2+} concentrations but are modified by the supply and loss of anions. Calculated flow-adjusted CO_2 consumption (**Fig. 1e**) peaked 2–3 years post-treatment with a broader peak in CO_2 consumption evident in 2007–2012 corresponding to declining legacy effects of acid rain until transient NO_3^- peaks appeared 2012–2015. The $\text{Wo-CO}_{2,\text{HCO}_3}$ shows a pattern that mirrors the $\text{Wo-CO}_{2,\text{Ca}}$ but is generally 5 times lower (**Fig. 1c,f**).

3.2 Sulphuric, nitric and organic acids reduce CDR

285 We next undertook sensitivity analyses to investigate the effects of acid deposition, increased NO_3^- and organic acid export from the treated watershed on bicarbonate concentrations and resulting CO_2 consumption (**Fig. 2**). In a ‘Low SO_4^{2-} ’ scenario (**Fig. 2a–c**), we sought to understand the effects of acid deposition by replacing the mean monthly time-series of streamwater and rainwater SO_4^{2-} for the treated watershed with a new time-series (purple curve, **Fig. 2a**) created by repeating the post-2010 datasets, which reflect diminished acid deposition following emission controls from the US Clean Air Act (Likens and Bailey, 290 2014). Removing acid rain effects in this manner dramatically increased the calculated bicarbonate concentrations and total annual CO_2 consumption ($\text{CO}_{2,\text{HCO}_3}$), increasing the initial spikes resulting from the wollastonite treatment in both by at least four-fold (purple curves, **Fig. 2 b,c**). An additional legacy of acidification in North American forests (Harrison et al., 1989) is SO_4^{2-} retention on soil clay mineral Fe and Al oxides (Fuller et al., 1987), which were subsequently released by increased soil pH following wollastonite weathering (Shao et al., 2016; Fakhraei et al., 2016). To assess the effect of this legacy SO_4^{2-} , we 295 ran simulations substituting the lower streamwater SO_4^{2-} concentrations from R in T (T REF, green curves, **Fig. 2b,c**). Results suggest that legacy SO_4^{2-} accounts for over half of the total acid deposition effect on increased $[\text{HCO}_3^-]_{\text{stream}}$ and CO_2 consumption in the simulations.

In the ‘Ref NO_3 ’ scenario (**Fig. 2 d–f**), seasonal spikes in streamwater export of NO_3^- recorded from the treated watershed between 2012 and 2015 were removed by substituting the reference watershed streamwater NO_3^- concentration measurements



300 lacking these spikes. This manipulation markedly increased modelled bicarbonate (**Fig. 2e**) and mean annual CO₂ consumption (**Fig. 2f**). To quantify the effects of organic acids on bicarbonate production in the treated watershed, we ran “+OA” and “-OA” simulations, i.e., with and without accounting for organic acids, respectively (**Fig. 2 g–i**). Results showed that removing OA from our simulations also increased modelled streamwater bicarbonate concentration (**Fig. 2h**), and resulting CO₂ consumption (**Fig. 2i**), in the treated watershed.

305 3.3 Effects of increasing wollastonite treatment

Because the HBEF application rate (3.44 t ha⁻¹) is smaller than the 10–50 t ha⁻¹ suggested for ERW strategies (Strefler et al., 2018; Beerling et al., 2018), we simulated the possible effects of a ten-fold increase in the streamwater Ca²⁺ concentrations on bicarbonate production (**Fig. 3a**) and CO₂ consumption (**Fig. 3b**). In this initial assessment, we assume streamwater responses are directly proportional to wollastonite application rate, i.e., 34.4 t ha⁻¹, and that all other variables remained unchanged. 310 Results show that after 15 years, cumulative Wo-CO_{2,HCO₃} is 73% of Wo-CO_{2,Ca} (**Fig. 3c**), as opposed to less than 20% for the actual rate of 3.44 t ha⁻¹ (**Table 2**). These results suggest that at higher application rates of wollastonite, the details of the CO₂ consumption calculations become less important.

3.4 Amplification of organic carbon sequestration by wollastonite treatment

In reversing long-term Ca²⁺ depletion of soils, the silicate rock treatment significantly increased forest growth and wood production between 2–12 years post-treatment relative to the reference watershed (Battles et al., 2014). This forest response increased total carbon sequestration by 20.7 mol C m⁻² or 9.1 t CO₂ ha⁻¹ during those ten years as a result of the treatment (Methods).

Changes in greenhouse gas (GHG) emissions from soils represent a further route to affecting the climate mitigation potential of the wollastonite treatment. Despite a rapid increase of one pH unit in the upper organic soil horizon (Oie), soil respiration CO₂ fluxes showed no significant difference between watersheds during the first three years after treatment (Groffman et al., 2006). However, our analysis of newly available longer-term datasets indicates that the treatment significantly reduced soil respiration in the high elevation hardwood zone (~660–845m a.s.l.) ($\chi^2(1,270)=17.2$, $P < 0.001$), possibly due to reduced fine-root biomass (Fahey et al., 2016) rather than changes in microbial activity (Groffman et al., 2006). No significant effects on soil respiration were detected in any of the other HBEF vegetation zones (**Fig. 4**). The wollastonite treatment increased the soil sink strength for CH₄ ($\chi^2(1,266)=30.8$, $P < 0.001$) in the low-elevation hardwood zone (482–565m a.s.l.), while it decreased in the high elevation zone ($\chi^2(1,268)=22.3$, $P < 0.001$) (SI Appendix, Fig. S8). There were no significant treatment effects on soil N₂O fluxes in any vegetation zone (SI Appendix).

3.5 Logistical CO₂ emissions and net CDR

Because the HBEF application rate (3.44 t ha⁻¹) is smaller than the 10–50 t ha⁻¹ suggested for ERW strategies (Strefler et al., 2018; Beerling et al., 2018), we simulated the possible effects of a ten-fold increase in the streamwater Ca²⁺ concentrations on



bicarbonate production (**Fig. 3a**) and CO₂ consumption (**Fig. 3b**). In this initial assessment, we assume streamwater responses are directly proportional to wollastonite application rate, i.e., 34.4 t ha⁻¹, and that all other variables remained unchanged. Results show that after 15 years, cumulative Wo-CO_{2,HCO₃} is 73% of Wo-CO_{2,Ca} (**Fig. 3c**), as opposed to less than 20% for the actual rate of 3.44 t ha⁻¹ (**Table 2**). These results suggest that at higher application rates of wollastonite, the details of the CO₂ consumption calculations become less important.

335

3.6 Potential for deployment at larger scales

The HBEF forests are representative of a major area of eastern North America receiving acid deposition since the 1950s (Likens and Bailey, 2014) which may be suitable for remediation and carbon capture via ERW treatment with a silicate rock or mineral. For example, the Appalachian and Laurentian-Acadian Northern Hardwood Forests (NHWF) covering a combined area of 0.137 Mkm² in the United States (Ferree and Anderson, 2013) have the same dominant hardwood trees as the HBEF experimental watersheds (*Fagus grandifolia*, *Betula allegheniensis* and *Acer saccharum*). Acid deposition exceeded “critical loads” likely to harm ecosystems in almost 9000 ha of New Hampshire’s *Acer saccharum* stands (NHAs) (Schaberg et al., 2010). These forests might be expected to respond similarly to a wollastonite treatment. The acid-sensitive trees *Acer saccharum* and *Picea rubens* are also widely distributed along the high elevation acid sensitive regions of the Appalachian Mountains which have already been impacted by acid deposition (Lawrence et al., 2015). We define this as a 40-km corridor along the Appalachian Mountains comprising 0.14 Mkm² and overlapping with the High Allegheny Plateau Ecoregion (HAL) where *Acer saccharum* is declining above ~550 m a.s.l. (Bailey et al., 2004) (0.07 Mkm²).

340

345

355

350

4 Discussion

Our analyses of wollastonite application at the HBEF provide a unique long-term (15 year) perspective on the whole watershed carbon cycle responses and net CDR by accounting for the associated CO₂ costs of logistical operations. By 2015, net CDR amounted to 8.5–11.5 t CO₂ ha⁻¹ at a low rate of wollastonite application, with increased carbon sequestration into forest biomass playing the dominant role. We estimate that if the HBEF application rates were increased ten-fold, net CDR would increase by 8%, assuming 400-km transport distances and no change in forest responses. Amplification of organic carbon



capture may therefore represent a major CDR benefit of ERW when applied to forested lands affected by acid rain. Forest management practices, disturbance regimes and the ultimate fate of any harvested wood are also important in determining the storage lifetime of the sequestered carbon. Our results highlight the need to carefully monitor the net carbon balance of forested
365 ecosystems in response to a silicate treatment, including wood and canopy respiration (Fahey et al., 2005) (Methods). This challenging goal might best be achieved with fully instrumented eddy covariance plots, although the HBEF topography is not well suited for this approach (Fahey et al., 2005).

Inorganic CO₂ consumption calculated based on streamwater bicarbonate fluxes approximately doubled in the treated watershed relative to the reference watershed 15 years post-treatment (0.028 and 0.016 tCO₂ ha⁻¹, respectively) (Table 1). The
370 presence of SO₄²⁻, NO₃⁻ and organic acid anions lowered the efficiency of CO₂ consumption by alkalinity generation, with acid deposition having the single largest calculated effect (Table 1). The cause of increased NO₃⁻ export from the treated watershed is not as yet understood (Rosi-Marshall et al., 2016). If it proves a general feature of terrestrial ecosystem responses to silicate mineral treatment, this could affect the efficiency of carbon capture via bicarbonate export. Overall, we suggest that continued recovery of eastern North American and European forests and soils from acid deposition creates conditions beneficial to
375 watershed health, carbonic acid-driven weathering and inorganic carbon export following application of crushed silicate minerals.

In Asia, acid rain is an ongoing problem with an estimated 28% of Chinese land area (~2.7 Mkm²) receiving potentially damaging S deposition in 2005 (Zhao et al., 2009), and critical loads were exceeded in ~0.36 Mkm² of the European Economic Area (EEA) in 1999 (Larssen et al., 2003), approximately double the affected area of US Northern Hardwood Forests (Fig. 6).
380 Fig. 6 suggests that a single 30t Wo ha⁻¹ treatment over 0.14 Mkm² (Appalachian Trail corridor) could, in principle, sequester ~1 MtCO₂ y⁻¹ or 15 MtCO₂ over 15 years via wollastonite-derived Ca export in streamwater alone. Adding the Chinese and European acidified areas could potentially sequester 0.34 GtCO₂, approximately 0.2–0.7% of the ~50–150 Gt CDR required by 2050 to avoid warming in excess of 1.5° (Rogelj et al., 2018). Inclusion of biomass and soil responses increases CDR contributions from ERW on acidified forests, but these will still be modest. Assuming no further forest responses beyond the
385 15-year HBEF timeframe, we report a GHG balance of ~10 tCO_{2e} ha⁻¹. This translates to 1 GtCO_{2e} Mkm⁻² suggesting 3.2 GtCO_{2e} over 15 years for the Appalachian Trail, the EEA and China combined, or 2–6% of global required CDR as described above.

It is uncertain whether other acidified forest ecosystems would respond similarly to the HBEF *Acer saccharum* forests in New Hampshire. Many Chinese soils (Duan et al., 2016), as well as old deep soils in areas such as the Virginian Blue Ridge
390 Mountains and the German Harz and Fethel Mountains (Garmo et al., 2014) have high SO₄²⁻ sorption capacity. These soils may retain substantially more SO₄²⁻ than the HBEF soils, with potential for prolonged SO₄²⁻ flushing following ERW treatment and lower bicarbonate production. Liming studies suggest a range of other effects, some of which may also occur with silicate treatments. Liming increases nitrate export, migration of heavy metals and acidity to deeper soil, and fine root production in topsoils leading to frost damage (Huettl and Zoettl, 1993).



395 Many forests have been limed with carbonate minerals such as calcite and dolomite to mitigate acidification in the past. Dolomite has also helped reverse Mg deficiency in conifers (Huettl and Zoettl, 1993). Liming generally improves water quality, although it also forms mixing zones with high-molecular-weight Al complexes toxic to fish (Teien et al., 2006). With silicate treatments, nontoxic hydroxyaluminosilicates form instead (Teien et al., 2006). Unfortunately, carbonates are contraindicated for CDR on acid soils because they can be a net source of CO₂ in the presence of strong acids (Hamilton et al., 400 2007). Treatments of European and North American acidified forests with calcite (1–18 t ha⁻¹ CaCO₃) or dolomite (2–8.7 t ha⁻¹ CaMg(CO₃)₂) have, in general, resulted in increased DOC export and soil respiration without increasing tree growth, regardless of forest composition (Lundström et al., 2003). As calcite and dolomite are 44% and 48% CO₂ by weight, these treatments will have released 0.44–7.9 and 0.96–4.54 t CO₂ ha⁻¹ respectively when fully dissolved, although dissolution may be slow. Over six years following a 2.9 t dolomite ha⁻¹ treatment (90% 0.2–2.0 mm grains) in a Norwegian coniferous 405 watershed equating to 1.36 t CO₂ ha⁻¹, less than 1% of the dolomite dissolved (Hindar et al., 2003). We estimate that CO₂ consumption corrected for CO₂ release and as measured with dolomite-derived Ca and Mg in streamwater (Dol-CO_{2,Ca+Mg}) averaged 0.02 mol CO₂ m⁻² yr⁻¹. CO₂ release from carbonate minerals equals Ca and Mg release on a molar basis, so 0.02 mol Dol-CO₂ m⁻² yr⁻¹ was also either exported in streamwater or lost to the atmosphere. This experiment may have a negative 410 greenhouse-gas balance depending on logistical penalties and soil respiration, as there was no significant treatment effect on tree growth or vitality (Hindar et al., 2003). Ca-sensitive *Acer saccharum* is present at Woods Lake in New York State, yet tree biomass decreased with no significant differences relative to reference catchments during the 20 years following a 6.89 t Mg-calcite ha⁻¹ application (Melvin et al., 2013), equivalent to 3.07 t CO₂ ha⁻¹ given 8% Mg content of the pellets. In contrast to our study and other liming studies, root biomass and soil carbon stocks increased in response to this treatment, although soil 415 respiration was reduced (Melvin et al., 2013). *Acer saccharum* basal area and crown vigour increased over 23 years in response to 22.4 t dolomitic limestone ha⁻¹ (equivalent to 10.0 t CO₂ ha⁻¹) on the Allegheny Plateau, although basal area and survival of another dominant canopy species, *Prunus serotina*, was reduced (Long et al., 2011). Clearly, forest responses to mineral 420 treatments are species- and site-specific.

Although the HBEF experiment used wollastonite, this is not a target mineral for ERW, both because of its limited reserves (Curry, 2019) and high monetary costs (Schlesinger and Amundson, 2018). Recent all-inclusive guide prices of ~700 USD Mg⁻¹ for helicopter deployment of pelletized lime along the Appalachian Mountain corridor are comparable to the price of 694 USD Mg⁻¹ for unpelletized 10-μm wollastonite in 2000 (Virta, 2000). Less expensive materials such as locally-sourced waste fines from mines should be considered if their heavy metal content is low, but the choice of treatment material should be considered together with the vegetation and the native minerals. Application of magnesium-rich materials (e.g. olivine), for example, may help reverse Mg deficiency in *Pinus sylvatica* and *Picea abies* as dolomite has done (Huettl and Zoettl, 425 1993), but some other tree species, such as *Acer saccharum*, have a higher demand for calcium than for magnesium (Long et al., 2009). The treatment of ecologically sensitive catchments always requires caution as some species, such as *Sphagnum* mosses and lichens, may respond poorly to treatment (Traaen et al., 1997).



5 Conclusions

This study identifies key challenges in accounting for CO₂ removal and feasibility for larger-scale rollout of ERW. Our two
430 methods for calculating the treatment effect on CO₂ consumption depend on strontium isotope data and a site-specific mixing model. At the HBEF, forest responses helped repay the initial carbon treatment penalties, but this depended on the presence of a Ca-sensitive species growing on soils stripped of calcium by decades of acid deposition. Given good access roads, helicopter deployment and pelletization may be unnecessary for application on land undergoing afforestation. Co-deployment of ERW with the CDR techniques favoured by the IPCC (Pachauri et al., 2014), afforestation and bioenergy with carbon dioxide capture
435 and storage (BECCS), may contribute to the twin aims of mitigating the effects of acid deposition on forests and CDR, but site-specific research is required to assess the efficacy and suitability of such strategies.

Code availability

The aqueous geochemistry software PHREEQC software, along with documentation, is freely available from the USGS website (<https://www.usgs.gov/software/phreeqc-version-3>). MATLAB® may be purchased from the MathWorks website
440 (<https://uk.mathworks.com/products/matlab.html>). the scripts used to process the HBEF data are available from the corresponding author, without guarantees that these will run with MATLAB versions other than R2016a.

Data availability

Our data are available from the Long Term Ecological Research (LTER) Network Data Portal. This public repository can be accessed via the Hubbard Brook Ecosystem Study website: <https://hubbardbrook.org/d/hubbard-brook-data-catalog>
445 See Supplement for a full list of filenames, package IDs, DOIs and access dates.

Author contributions

All authors contributed to project conceptualization and interpretation of model results. L.L.T. undertook model simulations and data analysis. L.L.T. and D.J.B. drafted the manuscript with edits and revisions from all authors. C.T.D. designed the wollastonite watershed study, provided data and observations for model simulations. J.D.B. provided strontium isotope
450 datasets. P.M.G. provided soil respiration, nitrous oxide and methane flux data.

Competing interests

The authors declare that they have no conflict of interest.



Disclaimer

Acknowledgements

455 L.L.T. and D.J.B. gratefully acknowledge funding from the Leverhulme Trust through a Leverhulme Research Centre Award (RC-2015-029). This manuscript is a contribution of the Hubbard Brook Ecosystem Study. Hubbard Brook is part of the Long-Term Ecological Research (LTER) network, which is supported by the National Science Foundation (DEB-1633026). L.L.T. thanks Ruth Yanai for a helpful discussion about vegetation, Fred Worrall for advice on flow adjustment and flux calculation, Peter Wade for advice on the initial PHREEQC setup and Andrew Beckerman and Evan DeLucia for constructive criticism
460 and advice on statistical modelling. We are grateful to Gregory Lawrence for information about applying lime treatments to the Appalachian Trail corridor.

References

Bailey, S., Horsley, S., Long, R., and Hallett, R.: Influence of edaphic factors on sugar maple nutrition and health on the Allegheny Plateau, *Soil Science Society of America Journal*, 68, 243–252, 2004.

465 Balogh-Brunstad, Z., Keller, C. K., Bormann, B. T., O'Brien, R., Wang, D., and Hawley, G.: Chemical weathering and chemical denudation dynamics through ecosystem development and disturbance, *Global Biogeochemical Cycles*, 22, GB1007, 10.1029/2007GB002957, 2008.

Battles, J. J., Fahey, T. J., Driscoll Jr, C. T., Blum, J. D., and Johnson, C. E.: Restoring soil calcium reverses forest decline, *Environmental Science & Technology Letters*, 1, 15–19, 2014.

470 Battles, J. J., Driscoll Jr, C. T., Bailey, S. W., Blum, J. D., Buso, D. C., Fahey, T. J., Fisk, M., Groffman, P. M., Johnson, C., and Likens, G.: Forest Inventory of a Calcium Amended Northern Hardwood Forest: Watershed 1, 2011, Hubbard Brook Experimental Forest. *Environmental Data Initiative*, 10.6073/pasta/94f9084a3224c1e3e0ed38763f8dae02, 2015a.

Battles, J. J., Driscoll Jr, C. T., Bailey, S. W., Blum, J. D., Buso, D. C., Fahey, T. J., Fisk, M., Groffman, P. M., Johnson, C., and Likens, G.: Forest Inventory of a Calcium Amended Northern Hardwood Forest: Watershed 1, 2006, Hubbard Brook Experimental Forest. *Environmental Data Initiative*, 10.6073/pasta/37c5a5868158e87db2d30c2d62a57e14, 2015b.

475 Beerling, D. J., Leake, J. R., Long, S. P., Scholes, J. D., Ton, J., Nelson, P. N., Bird, M., Kantzas, E., Taylor, L. L., and Sarkar, B.: Farming with crops and rocks to address global climate, food and soil security, *Nature plants*, 4, 138–147, 2018.

Blum, J. D., Klaue, A., Nezat, C. A., Driscoll, C. T., Johnson, C. E., Siccama, T. G., Eagar, C., Fahey, T. J., and Likens, G. E.: Mycorrhizal weathering of apatite as an important calcium source in base-poor forest ecosystems, *Nature*, 417, 729–731, 2002.

480 Blum, J. D.: Streamwater Ca, Sr and $^{87}\text{Sr}/^{86}\text{Sr}$ measurements on Watershed 1 at the Hubbard Brook Experimental Forest. *Environmental Data Initiative*, 10.6073/pasta/43ebc0f959780cf30b7ad53cc4a3d3e, 2019.

Brantley, S. L., Kubicki, J. D., and White, A. F.: Kinetics of water-rock interaction, 2008.

Campbell, J.: Hubbard Brook Experimental Forest (USDA Forest Service): Daily Streamflow by Watershed, 1956–present, 485 *Environmental Data Initiative*, 10.6073/pasta/727ee240e0b1e10c92fa28641bedb0a3, 2015.

Campbell, J.: Hubbard Brook Experimental Forest (USDA Forest Service): Daily Mean Temperature Data, 1955–present. *Environmental Data Initiative*, 10.6073/pasta/75b416d670de920c5ace92f8f3182964, 2016.

Campbell, J. L., Driscoll, C. T., Eagar, C., Likens, G. E., Siccama, T. G., Johnson, C. E., Fahey, T. J., Hamburg, S. P., Holmes, R. T., and Bailey, A. S.: Long-term trends from ecosystem research at the Hubbard Brook Experimental Forest, Gen. Tech. Rep. NRS-17. Newtown Square, PA: US Department of Agriculture, Forest Service, Northern Research Station. 41 p., 17, 490 2007.



Campbell, J. L., Rustad, L. E., Boyer, E. W., Christopher, S. F., Driscoll, C. T., Fernandez, I. J., Groffman, P. M., Houle, D., Kiekbusch, J., and Magill, A. H.: Consequences of climate change for biogeochemical cycling in forests of northeastern North America, *Canadian Journal of Forest Research*, 39, 264–284, 2009.

495 Cawley, K. M., Campbell, J., Zwilling, M., and Jaffé, R.: Evaluation of forest disturbance legacy effects on dissolved organic matter characteristics in streams at the Hubbard Brook Experimental Forest, New Hampshire, *Aquatic sciences*, 76, 611–622, 2014.

Chetelat, B., Liu, C.-Q., Zhao, Z., Wang, Q., Li, S., Li, J., and Wang, B.: Geochemistry of the dissolved load of the Changjiang Basin rivers: anthropogenic impacts and chemical weathering, *Geochimica et Cosmochimica Acta*, 72, 4254–4277, 2008.

500 Cho, Y., Driscoll, C. T., Johnson, C. E., Blum, J. D., and Fahey, T. J.: Watershed-level responses to calcium silicate treatment in a northern hardwood forest, *Ecosystems*, 15, 416–434, 2012.

Mineral Commodity Summaries: Wollastonite: <https://www.usgs.gov/centers/nmic/wollastonite-statistics-and-information>, access: 11 September, 2019.

De Klein, C., Novoa, R. S., Ogle, S., Smith, K. A., Rochette, P., Wirth, T. C., McConkey, B. G., Mosier, A., Rypdal, K., and 505 Walsh, M.: N₂O emissions from managed soils, and CO₂ emissions from lime and urea application, *IPCC guidelines for National greenhouse gas inventories*, prepared by the National greenhouse gas inventories programme, 4, 1–54, 2006.

Driscoll, C. T., Bailey, S. W., Blum, J. D., Buso, D. C., Eagar, C., Fahey, T. J., Fisk, M., Groffman, P. M., Johnson, C., Likens, G., Hamburg, S. P., and Siccama, T. G.: Forest Inventory of a Calcium Amended Northern Hardwood Forest: Watershed 1, 2001, Hubbard Brook Experimental Forest. Environmental Data Initiative, 10.6073/pasta/a2300121b6d594bbfcb3256ca1c300c8, 2015.

510 Driscoll, C. T.: Longitudinal Stream Chemistry at the Hubbard Brook Experimental Forest, Watershed 6, 1982–present. Environmental Data Initiative, 10.6073/pasta/0033e820ff0e6a055382d4548dc5c90c, 2016a.

Driscoll, C. T.: Longitudinal Stream Chemistry at the Hubbard Brook Experimental Forest, Watershed 1, 1991–present. Environmental Data Initiative, 10.6073/pasta/fcfa498c5562ee55f6e84d7588a980d2, 2016b.

515 Driscoll Jr, C. T., Bailey, S. W., Blum, J. D., Buso, D. C., Eagar, C., Fahey, T. J., Fisk, M., Groffman, P. M., Johnson, C., Likens, G., Hamburg, S. P., and Siccama, T. G.: Forest Inventory of a Calcium Amended Northern Hardwood Forest: Watershed 1, 1996, Hubbard Brook Experimental Forest. Environmental Data Initiative, 10.6073/pasta/9ff720ba22aef2b40fc5d9a7b374aa52, 2015.

Duan, L., Yu, Q., Zhang, Q., Wang, Z., Pan, Y., Larssen, T., Tang, J., and Mulder, J.: Acid deposition in Asia: emissions, 520 deposition, and ecosystem effects, *Atmospheric Environment*, 146, 55–69, 10.1016/j.atmosenv.2016.07.018, 2016.

Energy Information Administration: Energy-Related Carbon Dioxide Emissions by State, 2005–2016, United States Department of Energy, Washington DC 20585, 34, 2019.

Fahey, T., Siccama, T., Driscoll, C., Likens, G., Campbell, J., Johnson, C., Battles, J., Aber, J., Cole, J., and Fisk, M.: The 525 biogeochemistry of carbon at Hubbard Brook, *Biogeochemistry*, 75, 109–176, 2005.

Fahey, T. J., Heinz, A. K., Battles, J. J., Fisk, M. C., Driscoll, C. T., Blum, J. D., and Johnson, C. E.: Fine root biomass declined in response to restoration of soil calcium in a northern hardwood forest, *Canadian Journal of Forest Research*, 46, 738–744, 2016.

Fakhraei, H., and Driscoll, C. T.: Proton and aluminum binding properties of organic acids in surface waters of the northeastern US, *Environmental science & technology*, 49, 2939–2947, 2015.

530 Fakhraei, H., Driscoll, C. T., Renfro, J. R., Kulp, M. A., Blett, T. F., Brewer, P. F., and Schwartz, J. S.: Critical loads and exceedances for nitrogen and sulfur atmospheric deposition in Great Smoky Mountains National Park, United States, *Ecosphere*, 7, e01466, 2016.

Ferree, C., and Anderson, M. G.: A map of terrestrial habitats of the Northeastern United States: methods and approach, *Nature Conservancy*, 10, 31, 2013.

535 Fuller, R., Driscoll, C., Lawrence, G., and Nodvin, S.: Processes regulating sulphate flux after whole-tree harvesting, *Nature*, 325, 707–710, 1987.

Garmo, Ø. A., Skjelkvåle, B. L., de Wit, H. A., Colombo, L., Curtis, C., Fölster, J., Hoffmann, A., Hruška, J., Høgåsen, T., and Jeffries, D. S.: Trends in surface water chemistry in acidified areas in Europe and North America from 1990 to 2008, *Water, Air, & Soil Pollution*, 225, 1880, 10.1007/s11270-014-1880-6, 2014.

540 Goodale, C. L., and Aber, J. D.: The long-term effects of land-use history on nitrogen cycling in northern hardwood forests, *Ecological Applications*, 11, 253–267, 2001.



Groffman, P. M., Fisk, M. C., Driscoll, C. T., Likens, G. E., Fahey, T. J., Eagar, C., and Pardo, L. H.: Calcium additions and microbial nitrogen cycle processes in a northern hardwood forest, *Ecosystems*, 9, 1289–1305, 2006.

545 Groffman, P. M.: Forest soil: atmosphere fluxes of carbon dioxide, nitrous oxide and methane at the Hubbard Brook Experimental Forest, 1997–present. *Environmental Data Initiative*, 10.6073/pasta/9d017f1a32cba6788d968dc03632ee03, 2016.

Hamilton, S. K., Kurzman, A. L., Arango, C., Jin, L., and Robertson, G. P.: Evidence for carbon sequestration by agricultural liming, *Global Biogeochemical Cycles*, 21, GB2021, 10.1029/2006GB002738, 2007.

550 Harrison, R. B., Johnson, D. W., and Todd, D. E.: Sulfate adsorption and desorption reversibility in a variety of forest soils, *Journal of Environmental Quality*, 18, 419–426, 1989.

Hartmann, J., West, A. J., Renforth, P., Köhler, P., Christina, L., Wolf-Gladrow, D. A., Dürr, H. H., and Scheffran, J.: Enhanced chemical weathering as a geoengineering strategy to reduce atmospheric carbon dioxide, supply nutrients, and mitigate ocean acidification, *Reviews of Geophysics*, 51, 113–149, 2013.

Hindar, A., Wright, R. F., Nilsen, P., Larssen, T., and Högberget, R.: Effects on stream water chemistry and forest vitality after 555 whole-catchment application of dolomite to a forest ecosystem in southern Norway, *Forest Ecology and Management*, 180, 509–525, 2003.

Hu, M., Chen, D., and Dahlgren, R. A.: Modeling nitrous oxide emission from rivers: a global assessment, *Global change biology*, 22, 3566–3582, 2016.

560 Huettl, R. F., and Zoettl, H.: Liming as a mitigation tool in Germany's declining forests—reviewing results from former and recent trials, *Forest Ecology and Management*, 61, 325–338, 1993.

Jacobson, A. D., and Blum, J. D.: Relationship between mechanical erosion and atmospheric CO₂ consumption in the New Zealand Southern Alps, *Geology*, 31, 865–868, 2003.

Johnson, C. E., Driscoll, C. T., Blum, J. D., Fahey, T. J., and Battles, J. J.: Soil chemical dynamics after calcium silicate addition to a northern hardwood forest, *Soil Science Society of America Journal*, 78, 1458–1468, 2014.

565 Johnson, N. M., Driscoll, C. T., Eaton, J. S., Likens, G. E., and McDowell, W. H.: 'Acid rain', dissolved aluminum and chemical weathering at the Hubbard Brook Experimental Forest, New Hampshire, *Geochimica et Cosmochimica Acta*, 45, 1421–1437, 1981.

Köhler, S., Laudon, H., Wilander, A., and Bishop, K.: Estimating organic acid dissociation in natural surface waters using total 570 alkalinity and TOC, *Water Research*, 34, 1425–1434, 2000.

Larsen, S., Barrett, K. J., Fiala, J., Goodwin, J., Hagen, L. O., Henriksen, J. F., de Leeuw, F., Tarrason, L., and van Aalst, R.: Air quality in Europe, 2003.

Lawrence, G., Sullivan, T., Burns, D., Bailey, S., Cosby, B., Dovciak, M., Ewing, H., McDonnel, T., Minocha, R., and Rice, K.: Acidic deposition along the Appalachian Trail corridor and its effects on acid-sensitive terrestrial and aquatic resources: 575 results of the Appalachian Trail MEGA-transect atmospheric deposition effects study, National Park Service, Fort Collins, Colorado, 2015.

Likens, G.: Chemistry of Bulk Precipitation at Hubbard Brook Experimental Forest, Watershed 6, 1963–present. *Environmental Data Initiative*, 10.6073/pasta/8d2d88dc718b6c5a2183cd88aae26fb1, 2016a.

Likens, G.: Chemistry of Bulk Precipitation at Hubbard Brook Experimental Forest, Watershed 1, 1963–present. *Environmental Data Initiative*, 10.6073/pasta/df90f97d15c28daeb7620b29e2384bb9, 2016b.

580 Likens, G. E., Buso, D. C., Dresser, B. K., Bernhardt, E. S., Hall Jr, R. O., Macneale, K. H., and Bailey, S. W.: Buffering an acidic stream in New Hampshire with a silicate mineral, *Restoration Ecology*, 12, 419–428, 2004.

Likens, G. E.: Biogeochemistry of a forested ecosystem, 3 ed., Springer Science & Business Media, 208 pp., 2013.

Likens, G. E., and Bailey, S. W.: The discovery of acid rain at the Hubbard Brook Experimental Forest: a story of collaboration and long-term research, in: USDA Forest Service Experimental Forests and Ranges, Springer, 463–482, 2014.

585 Littlewood, I., Watts, C., and Custance, J.: Systematic application of United Kingdom river flow and quality databases for estimating annual river mass loads (1975–1994), *Science of the Total Environment*, 210, 21–40, 1998.

Long, R. P., Horsley, S. B., Hallett, R. A., and Bailey, S. W.: Sugar maple growth in relation to nutrition and stress in the northeastern United States, *Ecological Applications*, 19, 1454–1466, 2009.

Long, R. P., Horsley, S. B., and Hall, T. J.: Long-term impact of liming on growth and vigor of northern hardwoods, *Canadian 590 Journal of Forest Research*, 41, 1295–1307, 2011.



Lovett, G. M., Likens, G. E., Buso, D. C., Driscoll, C. T., and Bailey, S. W.: The biogeochemistry of chlorine at Hubbard Brook, New Hampshire, USA, *Biogeochemistry*, 72, 191–232, 2005.

Lundström, U., Bain, D., Taylor, A., and Van Hees, P.: Effects of acidification and its mitigation with lime and wood ash on forest soil processes: a review, *Water, Air and Soil Pollution: Focus*, 3, 5–28, 2003.

595 Martin, A. R., Doraisami, M., and Thomas, S. C.: Global patterns in wood carbon concentration across the world's trees and forests, *Nature Geoscience*, 10.1038/s41561-018-0246-x, 2018.

McLauchlan, K. K., Craine, J. M., Oswald, W. W., Leavitt, P. R., and Likens, G. E.: Changes in nitrogen cycling during the past century in a northern hardwood forest, *Proceedings of the National Academy of Sciences*, 104, 7466–7470, 2007.

600 Melvin, A. M., Lichstein, J. W., and Goodale, C. L.: Forest liming increases forest floor carbon and nitrogen stocks in a mixed hardwood forest, *Ecological applications*, 23, 1962–1975, 2013.

Mohseni, O., and Stefan, H.: Stream temperature/air temperature relationship: a physical interpretation, *Journal of hydrology*, 218, 128–141, 1999.

Moon, S., Chamberlain, C., and Hillel, G.: New estimates of silicate weathering rates and their uncertainties in global rivers, *Geochimica et Cosmochimica Acta*, 134, 257–274, 2014.

605 Négrel, P., Allègre, C. J., Dupré, B., and Lewin, E.: Erosion sources determined by inversion of major and trace element ratios and strontium isotopic ratios in river water: the Congo Basin case, *Earth and Planetary Science Letters*, 120, 59–76, 1993.

Nezat, C. A., Blum, J. D., and Driscoll, C. T.: Patterns of Ca/Sr and $^{87}\text{Sr}/^{86}\text{Sr}$ variation before and after a whole watershed CaSiO_3 addition at the Hubbard Brook Experimental Forest, USA, *Geochimica et Cosmochimica Acta*, 74, 3129–3142, 10.1016/j.gca.2010.03.013, 2010.

610 Pachauri, R. K., Allen, M. R., Barros, V. R., Broome, J., Cramer, W., Christ, R., Church, J. A., Clarke, L., Dahe, Q., and Dasgupta, P.: Climate change 2014: synthesis report. Contribution of Working Groups I, II and III to the fifth assessment report of the Intergovernmental Panel on Climate Change, IPCC, 2014.

Parkhurst, D. L., and Appelo, C.: User's guide to PHREEQC (Version 2): A computer program for speciation, batch-reaction, one-dimensional transport, and inverse geochemical calculations, US Geological Survey, Denver, 326 pp., 1999.

615 Peters, S. C., Blum, J. D., Driscoll, C. T., and Likens, G. E.: Dissolution of wollastonite during the experimental manipulation of Hubbard Brook Watershed 1, *Biogeochemistry*, 67, 309–329, 10.1023/B:BIOG.0000015787.44175.3f, 2004.

Rogelj, J., Shindell, D., Jiang, K., Fifita, S., Forster, P., Ginzburg, V., Handa, C., Kheshgi, H., Kobayashi, S., Kriegler, E., Mundaca, L., Séférian, R., and Vilariño, M.: Mitigation Pathways Compatible with 1.5°C in the Context of Sustainable Development, 2018.

620 Rosi-Marshall, E. J., Bernhardt, E. S., Buso, D. C., Driscoll, C. T., and Likens, G. E.: Acid rain mitigation experiment shifts a forested watershed from a net sink to a net source of nitrogen, *Proceedings of the National Academy of Sciences*, 113, 7580–7583, 2016.

Schaberg, P. G., Miller, E. K., and Eagar, C.: Assessing the threat that anthropogenic calcium depletion poses to forest health and productivity, US Department of Agriculture, Forest Service, Pacific Northwest and Southern Research Stations, Portland, OR, 37–58, 2010.

625 Schlesinger, W. H., and Amundson, R.: Managing for soil carbon sequestration: Let's get realistic, *Global Change Biology*, 00, 1–4, 10.1111/gcb.14478, 2018.

Sebestyen, S. D., Boyer, E. W., and Shanley, J. B.: Responses of stream nitrate and DOC loadings to hydrological forcing and climate change in an upland forest of the northeastern United States, *Journal of Geophysical Research: Biogeosciences*, 114, G02002, 2009.

630 Shao, S., Driscoll, C. T., Johnson, C. E., Fahey, T. J., Battles, J. J., and Blum, J. D.: Long-term responses in soil solution and stream-water chemistry at Hubbard Brook after experimental addition of wollastonite, *Environ. Chem.*, 13, 528–540, 2016.

Sims, R., Schaeffer, R., Creutzig, F., Cruz-Núñez, X., D'agosto, M., Dimitriu, D., Figueroa Meza, M., Fulton, L., Kobayashi, S., and Lah, O.: Transport, Cambridge University Press, Cambridge and New York, 2014.

635 Sopper, W. E., and Lull, H. W.: The representativeness of small forested experimental watersheds in northeastern United States, *International Association of Hydrological Sciences*, 66, 441–456, 1965.

Stamboliadis, E., Pantelaki, O., and Petrakis, E.: Surface area production during grinding, *Minerals engineering*, 22, 587–592, 2009.

640 Strefler, J., Amann, T., Bauer, N., Kriegler, E., and Hartmann, J.: Potential and costs of carbon dioxide removal by enhanced weathering of rocks, *Environmental Research Letters*, 13, 034010, 2018.



Teien, H.-C., Kroglund, F., Åtland, Å., Rosseland, B. O., and Salbu, B.: Sodium silicate as alternative to liming-reduced aluminium toxicity for Atlantic salmon (*Salmo salar* L.) in unstable mixing zones, *Science of the total environment*, 358, 151-163, 2006.

645 Traaen, T., Frogner, T., Hindar, A., Kleiven, E., Lande, A., and Wright, R.: Whole-catchment liming at Tjønnstrond, Norway: an 11-year record, *Water, Air, and Soil Pollution*, 94, 163-180, 1997.

Emissions & Generation Resource Integrated Database (eGRID): https://www.epa.gov/sites/production/files/2018-02/egrid2016_all_files_since_1996.zip, access: 25 October, 1999.

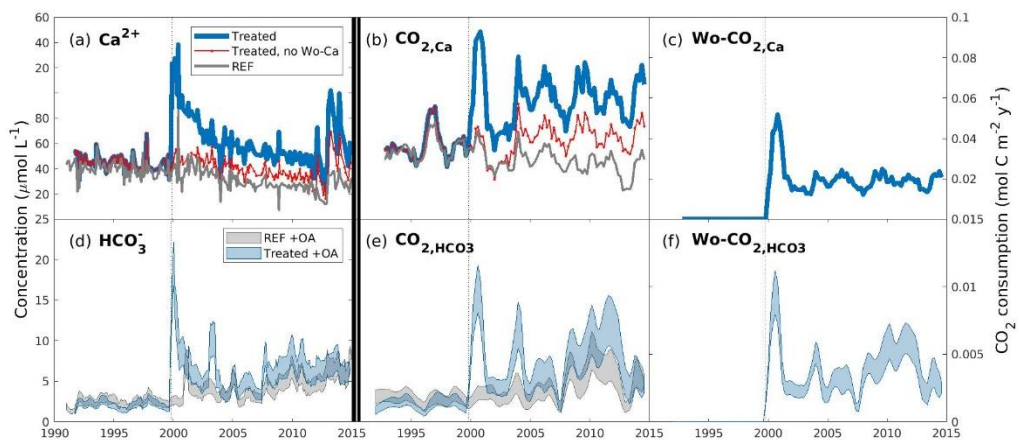
Minerals Yearbook: Wollastonite: <https://www.usgs.gov/centers/nmic/wollastonite-statistics-and-information>, access: 11 September 2000.

650 Zhao, Y., Duan, L., Xing, J., Larssen, T., Nielsen, C. P., and Hao, J.: Soil acidification in China: is controlling SO₂ emissions enough?, *Environmental Science & Technology*, 43, 8021-8026, 10.1021/es901430n, 2009.



Figures and Tables

655



660 **Figure 1: Inorganic CO₂ capture at the Hubbard Brook Experimental Forest.** (a) Observed calcium and (b) calcium export in the reference (grey) and treated (blue) watersheds along with the contribution from sources other than wollastonite (red). (c) Calculated CO₂ consumption due to the treatment (Wo-CO_{2,Ca}, Eq. 9). (d) Modelled streamwater bicarbonate, (e) CO₂ consumption (CO_{2,HCO₃}, Eq. 5), and (f) CO₂ consumption due to the treatment (Wo-CO_{2,HCO₃}, Eq. 7), colours as for calcium. Simulations (d–f) account for the presence of organic acids (+OA). All calcium export (b) and CO₂ consumption curves (c,e,f) were calculated with flow-normalised concentrations and corrected for sparsity of samples (Methods).

665

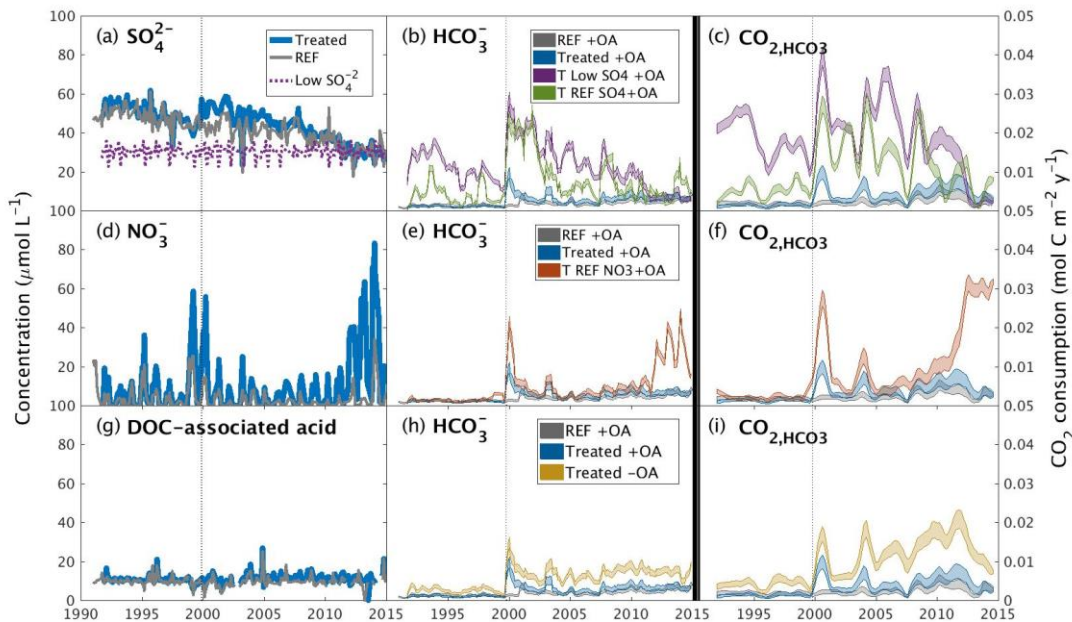


Figure 2: Sensitivity of watershed inorganic CO_2 capture at Hubbard Brook to environmental change. Modelled watershed streamwater bicarbonate and corresponding patterns of total CO_2 consumption ($\text{CO}_{2,\text{HCO}_3}$ by Eq. 5) and treatment-associated CO_2 consumption ($\text{Wo-}\text{CO}_{2,\text{HCO}_3}$ by Eq. 7) following (a–c) removal of acid deposition effects (“Low SO_4^2- ” scenario) or (d–f) removal of transient nitrate spiking (“REF NO_3^- ” scenario), and (g–i) sensitivity to the presence or absence of organic acids (OA^+ and OA^- , respectively). Bicarbonate concentrations (b,e,h) for all scenarios are shown to the same scale. All CO_2 consumption curves (c,f,i) are shown to the same scale and were calculated with flow-normalised concentrations and corrected for sparsity of samples (Methods).

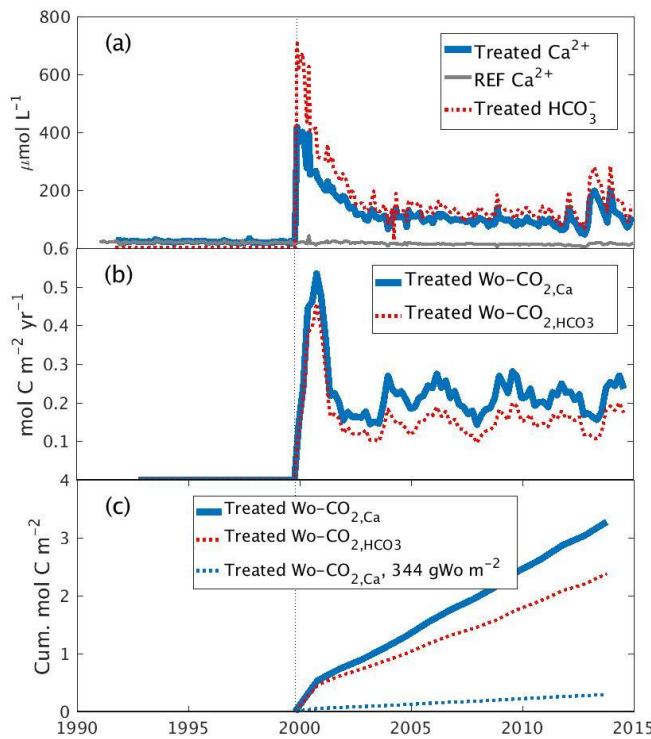


Figure 3: Simulated inorganic CO₂ capture for a 10-fold higher wollastonite treatment in the Hubbard Brook Experimental Forest.
675 (a) Calcium and bicarbonate concentrations, along with observed reference calcium. Calcium is charge-balanced by up to two moles of
bicarbonate. (b) CO₂ consumption due to this higher treatment (Wo-CO_{2,Ca} and Wo-CO_{2,HCO₃}) and (c) Cumulative CO₂ consumption for both
this higher treatment and the actual treatment (Wo-CO_{2,Ca}). We have assumed that a 10-fold higher treatment produces 10-fold higher calcium
concentrations with no change in sulphate, nitrate or DOC. Simulated HCO₃⁻ concentration and Wo-CO_{2,HCO₃} account for the presence of
680 organic acids (+OA) given observed DOC. All CO₂ consumption curves (b,c) were flow-normalised and corrected for sparsity of samples
(Methods).

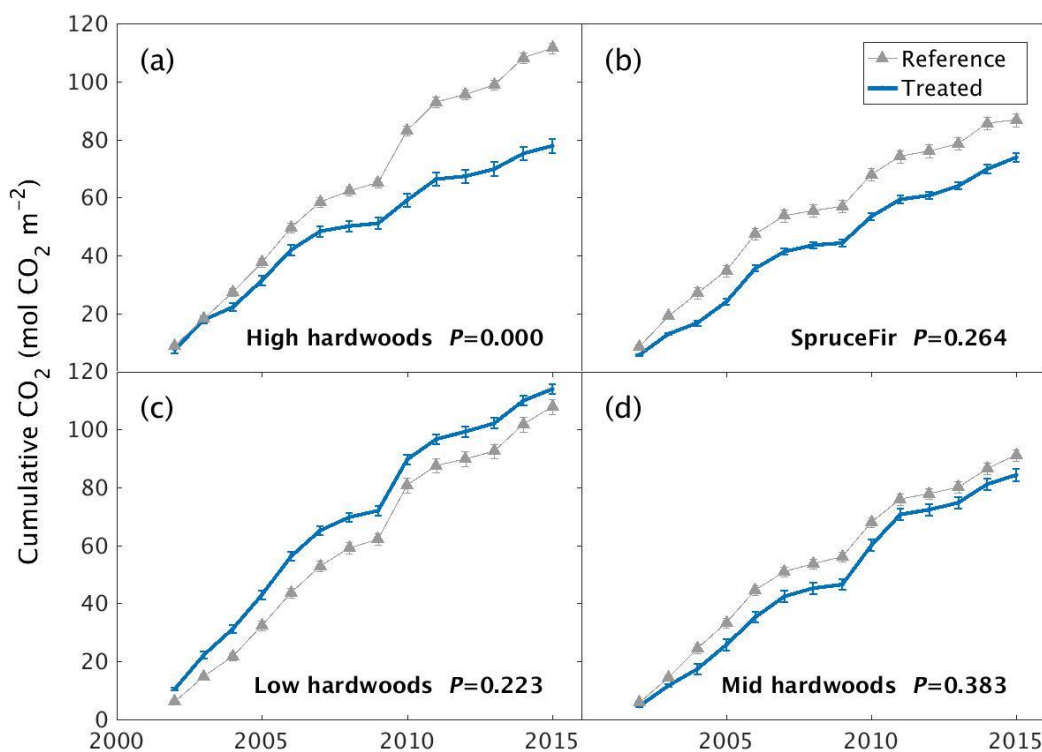


Figure 4: Long-term soil respiration responses to wollastonite treatment at Hubbard Brook Experimental Forest. Cumulative soil CO₂ respiration responses of treated and untreated (a) high elevation hardwoods, (b) high elevation conifers, (c) low elevation hardwoods or (d) mid-elevation hardwoods. Plots show cumulative means \pm 1 SE for three chamber measurements at each site and time. Reference data were collected from untreated forests immediately adjacent to the western edge of our reference catchment. P-values from Kruskal-Wallis tests comparing treated and reference raw data (SI Appendix) are shown.

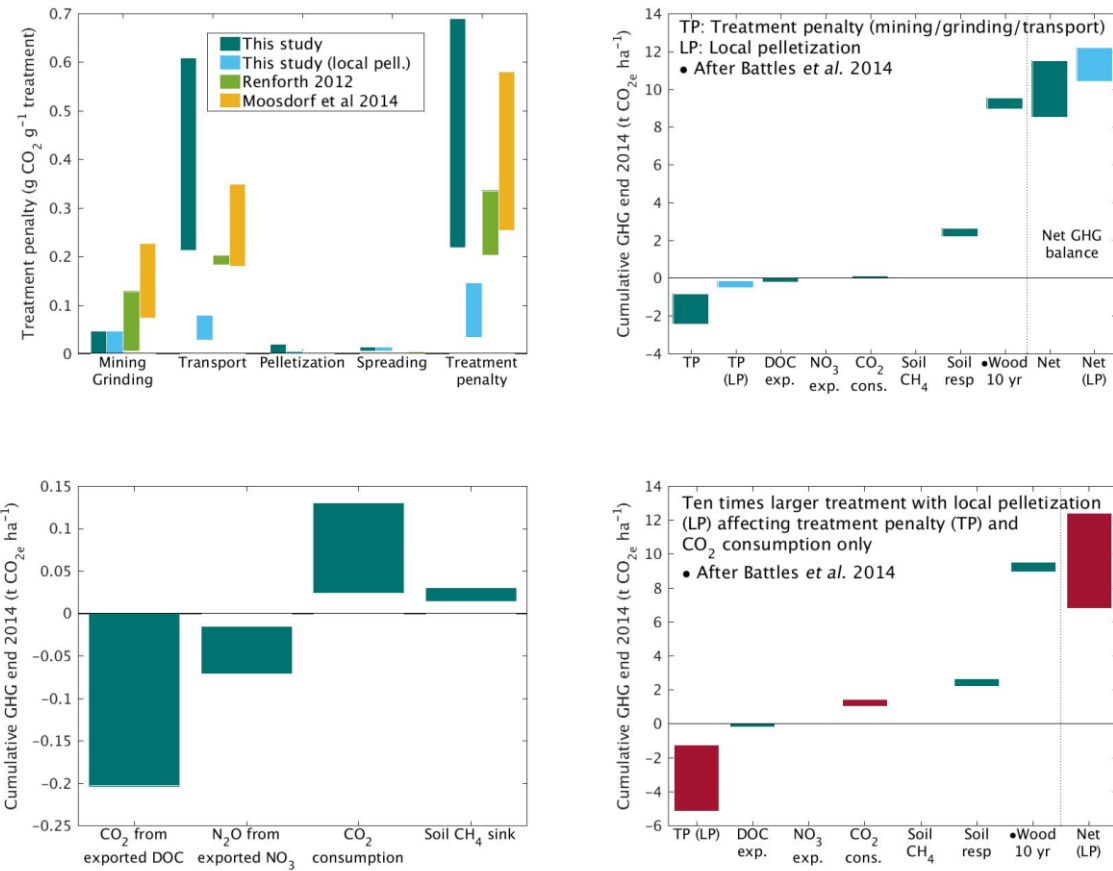


Figure 5: Carbon penalties and responses for the wollastonite treatment. (a) Carbon penalties for logistic elements of the treatment are compared with literature estimates for large-scale rollout of enhanced rock weathering for the HBEF treatment (3.44 t ha⁻¹). The wollastonite was shipped to Illinois for pelletization, so we also included estimates of the logistic penalties for local pelletization anywhere between the mine in Gouverneur, New York and the staging area in Woodstock, New Hampshire. (b) Elements of the greenhouse gas balance associated with the wollastonite treatment (Table 2). These include our calculated treatment effects at the end of 2014 along with the wood production produced over ten years published by Battles et al (Battles et al., 2014). The CO₂ consumption range is given by Wo-CO₂,HCO₃ calculated by Eq. (7) and Wo-CO₂,Ca calculated by Eq. (9). Nitrate export in streamwater leading to N₂O greenhouse gas emissions downstream and a small increase in the soil CH₄ sink have been converted to CO₂-equivalents (Methods). We found no significant effect for soil N₂O emissions. Exported DOC is assumed to be respired downstream. Note this is not a full greenhouse gas balance for the treatment as it neglects potential changes in large fluxes such as aboveground autotrophic respiration. (c) Smaller treatment effects from (b). (d) Elements of the greenhouse gas balance associated with a hypothetical ten-fold higher treatment. Here, we assume no change in forest or streamwater treatment responses other than CO₂ consumption.

690

695

700

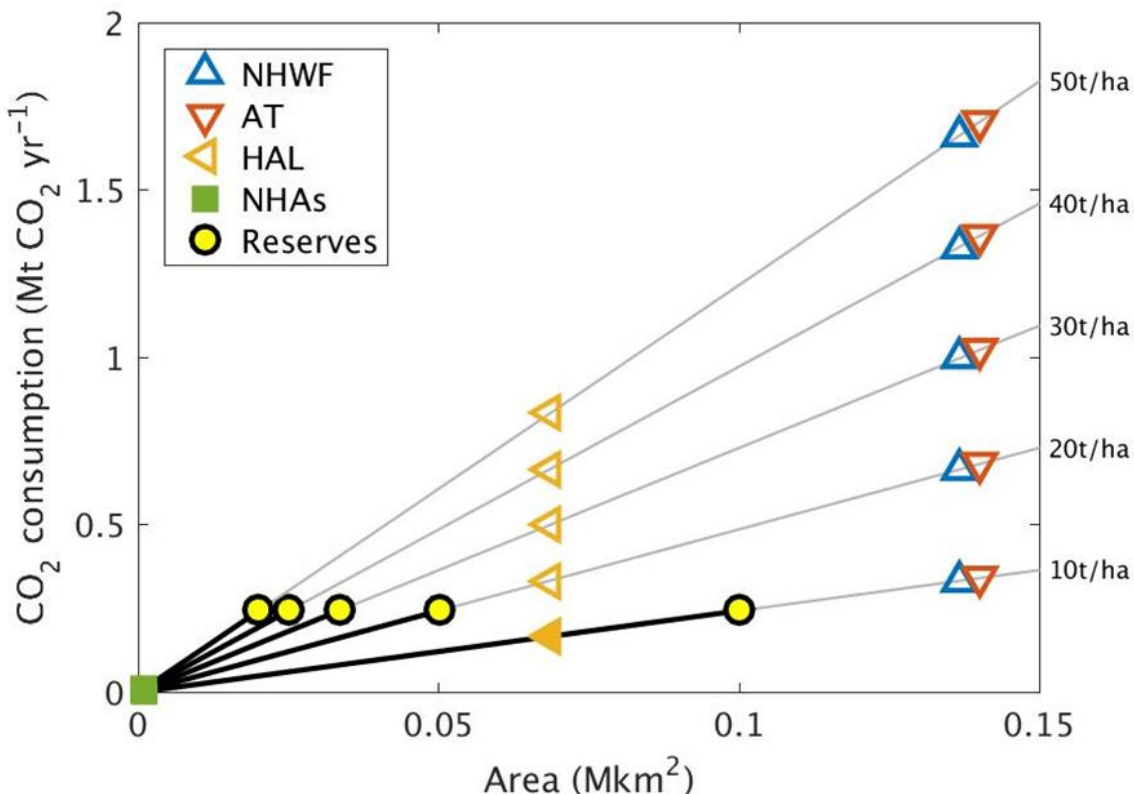


Figure 6: Projected CO₂ consumption following higher-dosage treatments. We considered the possibility of higher-dosage silicate treatments on other northeastern United States higher-altitude forests affected by acid rain, such as *Acer saccharum* forests in New Hampshire (NHAs), the High Allegheny Plateau Ecoregion (HAL), the Appalachian trail corridor (AT), or Northern Hardwood forests (NHWF) dominated by the same tree species as at Hubbard Brook. Because the world's wollastonite reserves (yellow disks) are insufficient to treat these areas, other calcium-rich silicate minerals would be required. CO₂ consumption due to higher dosage (t ha⁻¹) is estimated as: (mean observed CO_{2,Ca} between 2004 and 2012) × area × dosage / 3.44 t ha⁻¹.

705

Table 1. Cumulative fluxes from treatment date calculated with streamwater partial pressure of CO₂ (gas) = 3.63 × atmospheric CO₂ partial pressure measured at Mauna Loa (see Methods). DIC = dissolved inorganic carbon. Scenarios are defined in the main text.

Cumulative fluxes 1 year post-treatment date (19 October 2000)								
Watershed	Scenario	Org. acids	CO _{2,ions}	Wo-CO _{2,Ca}	DIC	HCO ₃	CO _{2,HCO₃}	Wo-CO _{2,HCO₃}
			(eqn 8)	(eqn 9)			(eqn 5)	(Eqn 7)
REF (6)	baseline	+OA	-0.003	0	0.084	0.002	0.002	0
Treated (1)	baseline	+OA	0.047	0.052	0.086	0.011	0.011	0.011
Treated (1)	baseline	-OA	0.047	0.052	0.094	0.019	0.019	0.018



Treated (1)	Low SO ₄	+OA	0.047	0.052	0.117	0.043	0.042	0.039
Treated (1)	REF NO ₃	+OA	0.102	0.052	0.105	0.030	0.030	0.029
Treated (1)	WoX10	+OA	0.513	0.534	0.533	0.457	0.457	0.457
Cumulative fluxes 15 years post-treatment (20 November 2014)								
Watershed	Scenario	Org. acids	CO _{2,ions} (eqn 8)	Wo-CO _{2,Ca} (Eqn 9)	DIC	HCO ₃	CO _{2,HCO3} (eqn 5)	Wo-CO _{2,HCO3} (Eqn 7)
mol C m ⁻²								
REF (6)	baseline	+OA	-0.274	0	1.307	0.052	0.036	0
Treated (1)	baseline	+OA	-0.044	0.294	1.299	0.083	0.064	0.057
Treated (1)	baseline	-OA	-0.044	0.294	1.414	0.198	0.179	0.145
Treated (1)	Low SO ₄	+OA	-0.044	0.294	1.523	0.307	0.270	0.179
Treated (1)	REF NO ₃	+OA	-0.044	0.294	1.410	0.194	0.175	0.127
Treated (1)	WoX10	+OA	2.600	3.275	3.626	2.406	2.387	2.380



715

Table 2. Elements of the ERW treatment carbon budget for the Hubbard Brook Experimental Forest wollastonite experiment.

Eqn 15	Carbon (t CO ₂ ha ⁻²)	Pessimistic	Optimistic
Ecosystem responses at the treatment site: $\Delta\text{NEP}^a + \Delta\text{CH4} - \Delta\text{N2O} - \Delta\text{TOC}^b$			
(Δwood)	Increased wood production over ten years relative to REF ^c	8.946	9.542
($-\Delta\text{TSR}$)	Reduced respiration since 2002 (whole forest) relative to REF	2.213	2.646
ΔCH4	Increased soil methane sink	0.015	0.029
ΔN2O	Increased soil N ₂ O emissions (not significant)	0	0
(ΔDOC^d)	DOC export penalty through 2014 relative to REF	-0.203	0
	Net ecosystem response at the treatment site through 2014	10.971	12.218
Downstream responses: $\Delta\text{CONS} - \Delta\text{NO3N2O}$			
ΔNO3N2O^d	Downstream N ₂ O penalty through 2014 relative to REF	-0.071	-0.016
ΔCONS	CO ₂ consumption through 2014 (Wo-CO _{2,HCO₃} and Wo-CO _{2,Ca})	0.025	0.129
	Net downstream balance through 2014	-0.046	0.113
Logistics: LOGPEN			
	Mining/Grinding given hydro or nuclear/petroleum power	-0.162	0
	Helicopter (~55 5-km flights)	-0.051	-0.021
	HDV transport (New York to Illinois to New Hampshire)	-2.135	-0.787
	Pelletization (in Illinois, coal power)	-0.068	0
LOGPEN	Total logistical penalty	-2.416	-0.808
	Partial greenhouse gas balance for the treatment	8.509	11.523

^aΔNEP, Net Ecosystem Productivity effect, is unknown, except for components Δwood and ΔTSR.

^bΔTOC=ΔPOC+ΔDOC. Possible increases in particulate organic carbon export (ΔPOC) are unknown.

^cAfter Battles et al. We have not attempted to extrapolate these results.

720 ^dΔTOC and ΔNO3N2O are penalties because these lead to CO₂ and N₂O emissions downstream

Table 3. Logistical penalty calculations for the Hubbard Brook wollastonite treatment

Penalty element	Value and calculation with units
Mass of wollastonite (CaSiO ₃) shipped to Allerton (t ^a Wo)	109665 lbs or 49.7432073 t Wo
Mass of pellets shipped from Allerton (t pellets)	112992 lbs or 51.2523091 t pellets
Ratio of pellet mass to Wollastonite mass	1.0368 = 51.25 t pellets / 49.74 t Wo
HDV transport distance (km)	3154 km = 1397 km (Gouverneur to Allerton) + 1757 km (Allerton to Woodstock)
Transport distance for “local pelletization” calculation (km)	408 km (Gouverneur to Woodstock)



Optimistic transport emissions (g CO ₂ g ⁻¹ Wo applied)	0.229 g CO₂ g⁻¹ Wo applied = 70 gCO ₂ km ⁻¹ shipped t ⁻¹ shipped × ((1397 km × 49.74 t Wo shipped)+(1757 km × 51.25 t pellets shipped)) / 48.86 × 10 ⁶ g Wo applied
Pessimistic transport emissions (g CO ₂ g ⁻¹ Wo applied)	0.620 g CO₂ g⁻¹ Wo applied = 190 gCO ₂ km ⁻¹ shipped t ⁻¹ shipped × ((1397 km × 49.74 t Wo shipped)+(1757 km × 51.25 t pellets shipped)) / 48.86 × 10 ⁶ g Wo applied
Mass of pellets deployed by helicopter (t pellets applied)	110992 lbs or 50.3451243 t pellets applied
Mass of wollastonite deployed by helicopter (t Wo applied)	48.86 t Wo applied = 50.345 t pellets applied / 1.03684
Total area treated (ha)	14.2 ha = 11.8 ha watershed plus 2.4 ha “destructive area” along the western edge
Nominal mean round trip flight distance (km, Woodstock to watershed and back)	5 km
Number of flights (1 short ton hopper capacity) ^b	55.5 = 50.345 t pellets / 0.907 t per trip
Molar mass of wollastonite CaSiO ₃ (g Wo mol ⁻¹ Wo)	116.17 g Wo mol⁻¹ Wo = 40.08 g Ca mol ⁻¹ Ca + 28.09 g Si mol ⁻¹ Si + 3 × 16 g O mol ⁻¹ O
Molar mass of CO ₂ (g CO ₂ mol ⁻¹ CO ₂)	44.01 g CO₂ mol⁻¹ CO₂ = 2 × 16 g O mol ⁻¹ O + 12.01 g C mol ⁻¹ C
Optimistic spreading emissions (mol CO ₂ ha ⁻¹)	483.36 mol CO₂ ha⁻¹ = 1200 gCO ₂ km ⁻¹ t ⁻¹ × 5 km × 50.345 t pellets / 44.01 g CO ₂ mol ⁻¹ CO ₂ / 14.2 ha
Optimistic spreading emissions (g CO ₂ g ⁻¹ Wo)	0.006 g CO₂ g⁻¹ Wo = 1200 gCO ₂ km ⁻¹ t ⁻¹ × 5 km × 50.345 t pellets / 48.86/10 ⁶ g Wo
Pessimistic spreading emissions (mol CO ₂ ha ⁻¹)	1168.1 mol CO₂ ha⁻¹ = 2900 gCO ₂ km ⁻¹ t ⁻¹ × 5 km × 50.345 t pellets / 44.01 g CO ₂ mol ⁻¹ CO ₂ / 14.2 ha
Pessimistic spreading emissions (g CO ₂ g ⁻¹ Wo)	0.015 g CO₂ g⁻¹ Wo applied = 2900 gCO ₂ km ⁻¹ t ⁻¹ × 5 km × 50.345 t pellets / 48.86 × 10 ⁶ g Wo applied

^aMegagrams or metric tons, not short tons

725 ^bNumber of flights does not explicitly enter into penalty calculations because the emissions for shorthaul aircraft are multiplied by the 5km round trip distance and the entire mass transported, rather than the mass transported during one round trip (one short ton).